

Seismic Design of Subsea Spools per ISO:

Part II- Seismic Requirements

Sirous F. Yasseri

Brunel University London; Sirous.Yasseri@Brunel.ac.uk;

ARTICLE INFO

Article History:

Received: 28 Aug. 2020

Accepted: 09 Dec. 2020

Keywords:

Subsea Spools

Soil- spool interaction

ISO 19902

ISO 19901

Earthquake

ALE and ELE

ABSTRACT

The ISO requires a two-level seismic qualification, namely Extreme Level Earthquake (ELE) and Accidental Level Earthquake (ALE) where damages that do not lead to leak is acceptable. ISO accepts both the response spectrum method and the time history approach. Since the spool-soil system behaves non-linearly, the time domain analyses must be performed for both levels. ISO requires 7 real earthquakes scaled for the site to be used for each seismic level and the system must pass at least 50% of the cases.

Best estimate soil models were developed to represent soil conditions at the manifolds locations in Part I. A set of 10 real earthquake time histories were propagated through the soil column for each location. The resulting ground motion at the surface was computed using a nonlinear model. The frequency-dependent ratio of spectra acceleration at the mudline to the stiff soil outcrop spectral acceleration (Spectral Amplification Ratio or SAR) was computed for each time history. The mean SAR was then used to modify the stiff soil hazard results from the PSHA to obtain design response spectra at the mudline.

This is the second part of three interlinked papers summarises the state of art for the benefit of practitioners of subsea engineering.

1. Introduction

This is the second part of a three-part paper dealing with the seismic design of subsea spools [32 and 33]. The seismic requirements for offshore structure design are covered in ISO 19901-2 and 19902. ISO balances the reliability and the potential consequences of undesirable performance. ISO methodology considers different soil, geologic conditions, and seismotectonic regions, and it is sensitive to input data and can account for the site characteristics uncertainties.

ISO requires each installation to withstand two earthquake intensity levels with prescribed acceptable performance. The first level is an Extreme Level Earthquake (ELE). The return period of the ELE depends on the commercial consequences of the installation's poor performance, which should have a reasonably low likelihood of being exceeded during the installation's service life. Installations should be designed so that little or no damage occurs when subjected to the ELE. Two objectives of the ELE design are,

- the ELE should ensure that the design is not susceptible to damage during relatively frequent seismic shaking at the site, and

- The design for ELE should endow enough strength reserve to minimize the design changes required to meet the performance criteria of the Abnormal Level Earthquake (ALE).

The second level is ALE, which is a rare, intense earthquake with a very low probability of being exceeded during the life of the installation. The ALE design check is performed using nonlinear analysis methods with the performance objective being the life safety and protection of the environment, but significant damage is acceptable. ISO criteria allow the use of a site-specific probabilistic seismic hazard analysis to define these two events. Doing this requires:

- Review geotechnical data for spools and manifold locations.
- Definition of soil amplification models for the manifold locations;
- Site response analysis to determine amplification/de-amplification of ground motion for ALE and 10,000 year return periods;
- Utilize amplification factors to define elastic response spectra at mudline for ALE and

10,000 year return periods. Define ELE mudline spectra based on Cr factor;

- Extract amplified acceleration time histories at mudline, and 15 m and 30 m below seafloor acceleration for the manifold location.

The method of analysis is straightforward. Best estimate soil models were developed to represent soil conditions at manifold locations. A set of 10 real earthquake time histories were propagated through the soil column for each location. The resulting ground motion at the surface was computed using a nonlinear model. The frequency-dependent ratio of spectra acceleration at the mudline to the stiff soil outcrop spectral acceleration (Spectral Amplification Ratio or SAR) was computed for each time history.

The mean SAR was then used to modify the stiff soil hazard results from the PSHA to obtain design response spectra at the mudline. As SAR is nonlinear with the intensity of ground shaking, the analysis is repeated for each return period scaling the input time histories of the target stiff soil PGA.

Acceleration time histories were also developed for the design. Seven earthquake accelerograms were considered. The horizontal components of the records were propagated through the soil profile and the corresponding motions extracted at mudline, 15 m, and 30 m penetration. The vertical motions are not expected to be significantly altered by the soil column and the original motions may be considered. The horizontal and vertical components were then scaled to the design elastic response spectra in the range of fundamental period of the structure (1 to 3 s for horizontal, 0.50 to 0.75 s for vertical). Time history data are provided for the ELE, ALE, and 10,000 year return periods.

2. ISO19902 Methodology

Annex B of ISO 1992-2 contains 1,000-year rock outcrop spectral acceleration associated with a single degree of freedom oscillator period of 0.2s and 1.0 second for worldwide locations. This information is used to determine the seismic load, especially for those sites that the simplified seismic design and analysis are acceptable. The site seismic zone is then determined from Table 1. Spectral acceleration $S_{a,map}(1.0)$ as shown in the ISO Worldwide Seismic Maps [ISO 19902-2 [16]] is used to define the site seismic zone.

Table1: Site Seismic Zone according to ISO 19902-2 [16]

| $S_{a,map}(1.0)$ | < 0,03 g | 0,03 g to 0,10 g | 0,11 g to 0,25 g | 0,26 g to 0,45 g | > 0,45 g |
|------------------|----------|------------------|------------------|------------------|----------|
| Seismic zone | 0 | 1 | 2 | 3 | 4 |

ISO then requires deciding the exposure level according to Table 2. The installation exposure level is defined in terms of the target annual probability of failure. Here, L1 is for the high consequence and L3 is for low consequence failure and if there is no pollution potential. (L2 is being removed in the updated code.)

Table 2: Relationship between exposure level and the annual probability of failure (Table 1 of ISO)

| Exposure level | P_f (annual probability of failure) |
|----------------|---------------------------------------|
| L1 | $4 \times 10^{-4} = 1 / 2,500$ |
| L2 | $1 \times 10^{-3} = 1 / 1,000$ |
| L3 | $2.5 \times 10^{-3} = 1 / 400$ |

Table 3 defines the seismic risk categories using the exposure level and the seismic zone category.

Table3: Seismic Risk Categories (ISO 19901-2)

| Site seismic zone | Exposure level | | |
|-------------------|----------------|-------|-------|
| | L3 | L2 | L1 |
| 0 | SRC 1 | SRC 1 | SRC 1 |
| 1 | SRC 2 | SRC 2 | SRC 3 |
| 2 | SRC 2 | SRC 2 | SRC 4 |
| 3 | SRC 2 | SRC 3 | SRC 4 |
| 4 | SRC 3 | SRC 4 | SRC 4 |

There is no requirement to conduct a seismic evaluation and for the risk category SRC 1 and SRC 2, thus the simplified method can be used. The standard procedure that adapts a standardized seismic hazard graph (Figure 2 of ISO 19902 [16]- the Code's response spectrum) can be used which simplifies calculations. For SRC 3 case, either the simplified or the detailed approach may be used. Depending on the seismic risk category the simplified method may produce a conservative design, thus it is best to use the detailed method. For SRC 4 the detailed method must be used.

For structures that are classified as seismic risk Category 3 or 4, it is recommended that the design response acceleration spectra be developed by detailed probabilistic seismic hazard analysis.

3. Probabilistic Seismic Risk Assessment

The probabilistic seismic assessment consists of the following elements:

- Development of earthquake **source-zonation** models
- Development of **earthquake recurrence relationships** and maximum magnitudes for each earthquake source zone
- Selection of appropriate **strong-motion attenuation** relationships
- Explicit incorporation of aleatory (randomness) and epistemic (modeling) **variability and uncertainty**
- **Probabilistic seismic hazard analyses** (PSHA)
- Development of generic and site-specific seismic design criteria

These elements are summarized below and in the flow chart given in Figure 1. The first three elements represent what is referred to as a seismotectonic model.

SEISMIC DESIGN CRITERIA METHODOLOGY

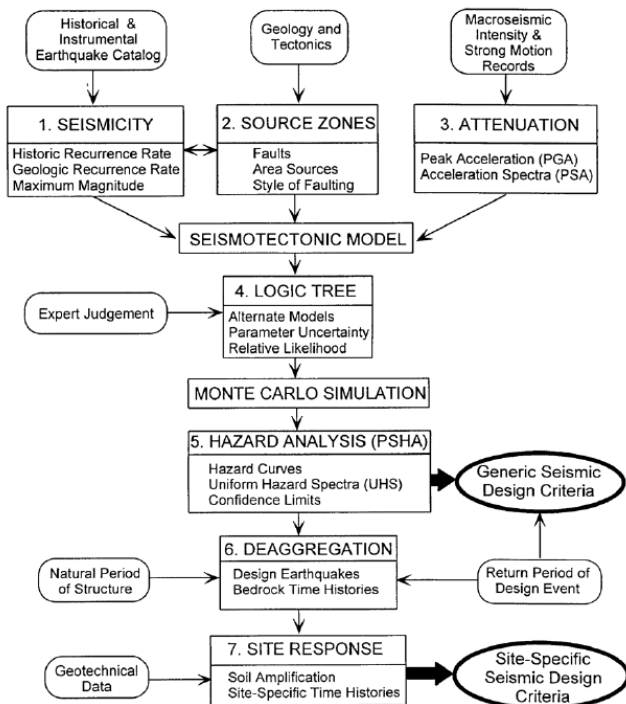


Figure 1: Flow chart showing the elements of the seismic design criteria methodology

3.1. Earthquake Source Zonation

Earthquake source zones are faults or seismotectonic provinces in which earthquakes are assumed to occur randomly with the same rate per unit length for fault sources or rate per unit area for area sources. The development of earthquake source zones entails identifying seismogenic sources—active faults or regions of diffuse seismicity. These sources are modeled as either individual faults or areas of similar seismicity and tectonic setting. Individual faults are modeled as three-dimensional vertical or dipping planes to properly account for the distribution of earthquake rupture with depth. Area sources also contain model faults that are assumed to be uniformly distributed concerning location and orientation (i.e. strike). Seismogenic sources are identified from information on the geology, tectonics, and historical seismicity of the region.

3.2. Earthquake Recurrence Relationship

Earthquake recurrence relationships quantify the frequency and size of earthquakes that are expected to occur in each earthquake source zone. Earthquake recurrence rates are estimated using the truncated exponential recurrence relationship originally proposed by Cornell and Vanmarcke [5].

Maximum magnitudes for individual faults are computed from relationships between earthquake magnitude and rupture dimensions developed by Wells and Coppersmith [31]. Maximum magnitudes for the area or distributed fault sources are estimated from historical seismicity, regional tectonics, the maximum lengths of mapped faults.

3.3. Strong Motion Attenuation

Attenuation relationships are used to predict strong ground-motion parameters from earthquake source and wave-propagation characteristics in the region of interest. The selected attenuation relationships are chosen to represent as closely as possible the tectonic environment of the earthquake source regions and the local site conditions of interest. An appropriate reference site condition is chosen for each site of interest to select a specific set of attenuation relationships to use in the seismic hazard analysis

3.4. Variability and Uncertainty

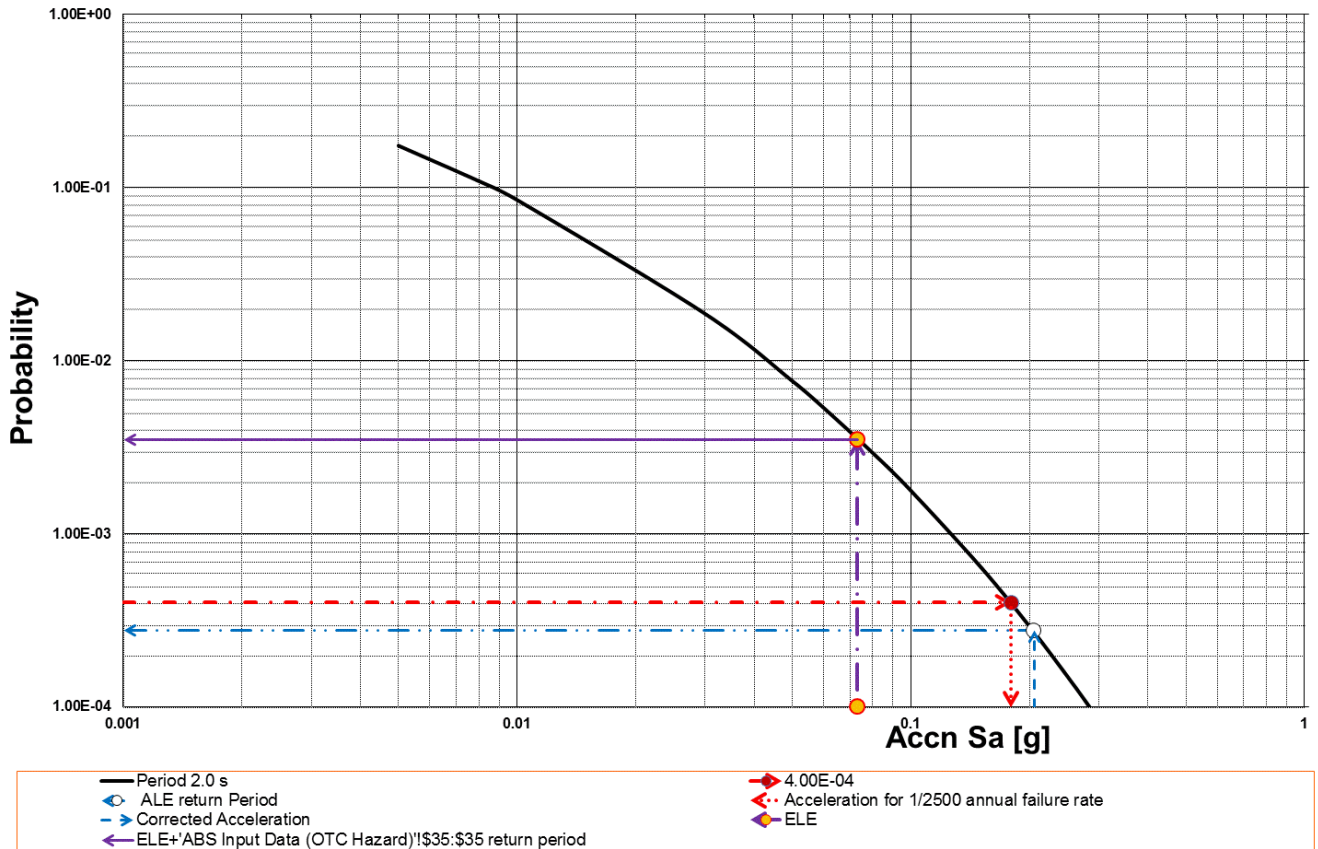
There are two types of variability—aleatory and epistemic—that can be included in a PSHA. Aleatory variability accounts for randomness associated with the size, location, and frequency of earthquakes together with other random effects inherent to the prediction of a parameter from a specific model assuming that the model is correct. Modeling uncertainty is a primary reason for inadequate predictive models and the variability in the employed data used for the models. Aleatory variability is included directly in the PSHA calculations utilizing mathematical integration. PSHA includes epistemic uncertainty which is done by explicitly including alternative hypotheses and models through the construction of a logic tree, and sampling the logic tree by a simulation method such as the Monte Carlo approach.

Each alternative hypothesis in the logic tree is given a subjective weight corresponding to its estimated likelihood of being correct. These alternative hypotheses will account for uncertainty in earthquake source zonation, maximum magnitude, recurrence rate, location and segmentation of seismogenic faults, type of faulting, distribution of seismicity between faults and area sources, as well as the ground-motion attenuation relationships[29].

3.5. Probabilistic Seismic Hazard Analysis (PSHA)

The hazard or probability of exceedance of a specified value of ground motion is calculated for each alternative hypothesis and set of model parameters selected utilizing Monte Carlo sampling of the logic-tree using a computational methodology similar to that first proposed by Cornell [6].

ISO acceleration - probability



ISO 19902 and ISO 19901-2 Return Period Derivation

NB: Assumed Values

Exposure Levels L1, L2 and L3 : L1 SD-Alpha Tdom = ~ 7 secs (?)
 Section 6.6 and Table 6.6.1, p. 20 to 22 L1 SD-Beta Tdom = ~ 4 secs (?)
 L2 - L3 (?) Manifold Tdom = ~ 0.5 secs (?)

Ref: "ISO Seismic Design Guidelines for Offshore Platforms"
 Banon, H., Cornell, C.A., Crouse, C.B., Marshall, P.W. and Nadim, F.
 20th Offshore Mechanics and Arctic Engineering Conf. - OMAE 2001
 Rio de Janeiro, Brazil, 3rd - 8th June 2001

(Ref. Cooper, 2005)

Notes: Pf = Probability of Failure

SRC = Seismic Risk Category

aR = Seismic Hazard Curve Slope ISO 19901-2 Figs 4 [a&b] p. 20 & 21

Cc = Correction Factor ISO 19901-2 Table 10 p. 19

Cr = Seismic Reserve Capacity Factor ISO 19902 Table 11.3.1 p. 61

Tdom = Structure Dominant Modal Period ISO 19901-2 Sec. 8.4 p. 19

$$Sa, ALE (Tdom) = Cc * Sa, pf (Tdom)$$

$$Sa, ELE (Tdom) = Sa, ALE (Tdom) / Cr$$

Refs. 1. BS EN ISO 19901-2: Petroleum and Natural Gas Industries - Specific Requirements for Offshore Structures — Part 2: Seismic Design Procedures and Criteria
 2. BS EN ISO 19902: Petroleum and Natural Gas Industries - Fixed Steel Offshore Structures

ISO 19902 and 19901-2 Input Constants ISO 19901-2 Site Seismic Zone 3

| ISO 19901-2 Exposure Level | pf | SRC | aR [0,5 s] | Cc [0,5 s] | aR [4,0 s] | Cc [4,0 s] | Cr | ISO Class; Tdom | Sa, pf | Sa, ALE | Sa, ELE | ALE RP | ELE RP |
|----------------------------|--------------------------------|-----|------------|------------|------------|------------|-----------|-----------------|--------|---------|---------|---------------------------------|---------------------------------|
| L1 | 4 x 10 ⁻⁴ = 1/2 500 | 4 | 1.80 | 1.19 | 2.15 | 1.141 | 2.8 [2.4] | L1; 4.0 secs | 0.068g | 0.074g | 0.0260g | 2.8 x 10 ⁻⁴ = 1/3600 | 3.3 x 10 ⁻³ = 1/300 |
| | | | | | | | | L1; 4.0 secs | 0.068g | 0.074g | 0.0308g | 2.8 x 10 ⁻⁴ = 1/3600 | 2.20 x 10 ⁻³ = 1/450 |
| | | | | | | | | L1; 2.0 secs | 0.170g | 0.202g | 0.072g | 3.0 x 10 ⁻⁴ = 1/3300 | 3.5 x 10 ⁻³ = 1/285 |
| | | | | | | | | L1; 2.0 secs | 0.170g | 0.202g | 0.084g | 3.0 x 10 ⁻⁴ = 1/3300 | 2.6 x 10 ⁻³ = 1/385 |
| L2 | 1 x 10 ⁻³ = 1/1 000 | 3 | 1.90 | 1.17 | 2.30 | 1.132 | 2.5 | L2; 0.5 secs | 0.400g | 0.468g | 0.187g | 6.7 x 10 ⁻⁴ = 1/1500 | 6.7 x 10 ⁻³ = 1/150 |
| L3 | 2.5 x 10 ⁻³ = 1/400 | 2 | 2.00 | 1.15 | 2.65 | 1.114 | 2.0 | L3; 0.5 secs | 0.280g | 0.322g | 0.161g | 2 x 10 ⁻³ = 1/500 | 1 x 10 ⁻² = 1/100 |

Figure 2: Typical Seismic Hazard Curve for T = T_{dom}

The input to the PSHA analyses is selected using the Monte Carlo simulation. The results of the simulations are then used to determine ground-shaking amplitudes and response spectra for specified fractiles as a function of the return period. Because of the complexity of the calculations, the probabilistic seismic hazard analyses are performed using a computer software package specifically developed to be used with a logic-tree formulation.

3.6. Re-aggregation of PSHA Results

The development of time histories for input to the dynamic site-response analysis requires knowledge of the magnitudes and distances that dominate the calculated ground-shaking hazard at the return periods and structural periods of interest. These magnitudes and distances define the design earthquakes and are determined from a process referred to as “de-aggregation.” For this purpose, the hazard for a given return period is partitioned into several magnitudes and distance bins. Then the relative contribution to the hazard in each bin is determined by the division of the bin exceedance frequency and the total exceedance frequency of all bins. The ‘mode’ is the bins with the largest relative contributions, that identify those earthquakes that are the largest contributors to the total

hazard. If no clear modes emerge as the dominant one, then the design earthquakes are generally defined by the mean magnitude and mean distance. Time histories are then chosen that are consistent with the magnitudes and distances of these design or controlling earthquakes[29].

The PSHA results are “de-aggregated” to determine the magnitudes and distances that contribute to the calculated exceedance frequencies (i.e., the hazard) for a given return period. These results are typically displayed as a histogram giving the percent contribution to the specified hazard of those earthquakes that are capable of causing ground motions equal to or greater than corresponding to this hazard as affected by the magnitude and distance [29].

Such histograms would be distinct for spectral accelerations of varying structural periods due to the difference in the way these spectral values scale with magnitude and distance [29]. The relative frequencies specified by these histograms are used to develop mean estimates of magnitude and distance to define a set of controlling or design earthquakes corresponding to specified structural periods and return periods. These design earthquakes are then used to select bedrock time histories for use in a dynamic site-response analysis or ground-failure evaluation.

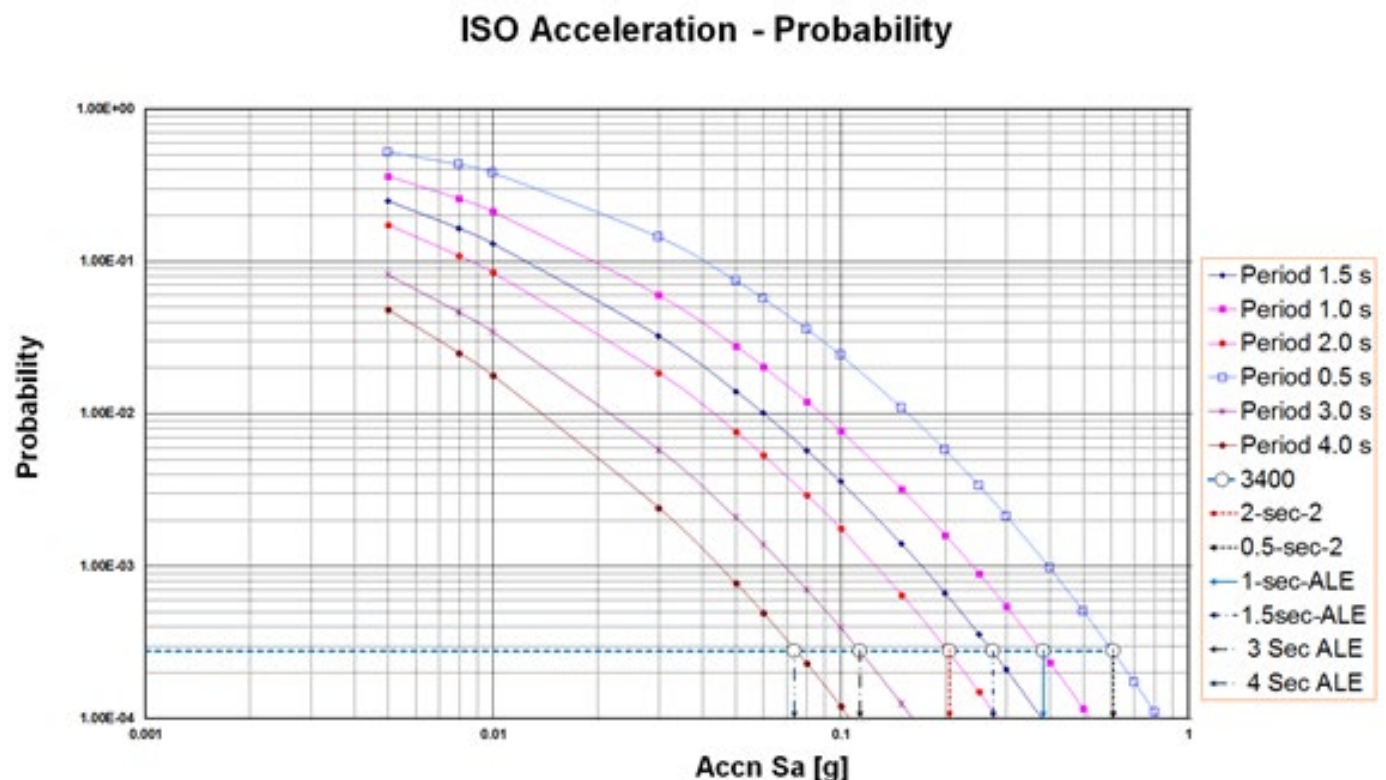


Figure 3: ISO Acceleration - Probability

4. Uniform Hazard Spectra

The design response spectrum for abnormal level earthquake and extreme level earthquake are derived

using the uniform hazard response spectrum (UHS), which is explained in the next section. The dominant modal period of the structure to be designed, T_{dom} , is determined first. The site-specific mean uniform

hazard spectral accelerations for T_{dom} , is plotted on a logarithmic scale (Figure2) This plot is used to determine the site-specific spectral acceleration at P_f , S_a , $P_f(T_{dom})$. The slope of the tangent at P_f termed a_R , is defined as the ratio of the spectral accelerations corresponding to two probabilities that are on either side of P_f and which are one order of magnitude apart, P_1 & P_2 , as seen in Figure 3.

The ISO procedures are as follows:

- For the given dominant period, T_{dom} , 2 seconds for the (or use 1.0 s if T_{dom} is not available) spool considered, the curve of exceedance probability $Pe(S_a)$ as a function of response acceleration S_a is plotted in log-log scale as shown in Figure 3.
- For the selected exposure level (L1), the failure probability p_f is defined (i.e., 1/2500).
- At $p_e = p_f$, the ratio (a_R) of S_{a1} (with probability exceedance of $p_1=E-4$) to S_{a2} (with probability exceedance of $p_2=E-3$) is determined such that $p_2/p_1 = 10$ and $p_1 < p_f < p_2$.
- A correction factor, C_c , is introduced per the value of a_R as per ISO (Table 4).
- At the dominant period, T_{dom} , the ALE response spectrum value $S_{A,ALE} = C_c S_a$ (with probability exceedance of p_f). The annual probability of exceedance for the ALE can be read from the seismic hazard curve or uniform seismic response spectra.
- At the spool's dominant period, T_{dom} , the ELE response spectrum value $S_{A,ELE} = S_{A,ALE}/C_r$. The annual probability of exceedance for the ELE can be read from the seismic hazard curve or uniform seismic response spectra. C_r is the seismic reserve capacity.
- Based on the determined annual probability of exceedance for the ELE or ALE, the uniform hazard response spectra $S_{A,ELE(T)}$, and $S_{A,ALE(T)}$ are determined.

Table 4 Correction factor C_c (Table 3-6 of ISO 1990-2)

| | | | | | |
|--------------------------|------|------|------|------|------|
| a_R | 1,75 | 2,0 | 2,5 | 3,0 | 3,5 |
| Correction factor, C_c | 1,20 | 1,15 | 1,12 | 1,10 | 1,10 |

Table 3-6. Correction Factor, C_c [ISO 19901-2].

5. Static and Dynamics Soil properties

The ground response to seismic shaking depends on the stiffness of the soil column, as well as the nonlinear decay of stiffness and level of damping versus strain developed during the seismic event. In terms of site response, the main parameters to be defined are:

- Soil unit weight;
- Shear modulus at small strain G_{max} , or equivalently the shear wave velocity V_s ;
- Decay of shear stiffness with the strain;

- Soil damping properties.

The submerged unit weight is a key parameter for the effective stress site response analysis. The small strain shear modulus (G_{max}) strongly influences the dynamic response of the soil column. The evaluation of G_{max} was based on the results of in-situ and laboratory testing. The small strain shear modulus (G_{max}) is related to the shear wave velocity (V_s) and soil density (ρ) as:

$$G_{max} = \rho V_s^2 \quad (1)$$

Laboratory results are compared to modulus decay and damping curves proposed by Vucetic and Dobry [30] for zero plasticity index, Ishibashi, and Zhang [17] and the low, average, and high curves suggested by Seed et al. [28]. The Vucetic and Dobry [30] curve is seen to provide the best match to the laboratory data. It was asserted by many researchers that laboratory tests indicate damping ratios rapidly decreases if shear strains are higher than about 1%. This behavior is consistent with the findings of Matasovic and Vucetic [22 and 23]. These authors have shown that at large strains sand tends to exhibit a dilatative behavior, then the hysteresis loop is no longer elliptical and the tendency of the stress-strain curve (the so-called "S shaping") leads to a rapid drop of hysteretic damping. For each applied cyclic stress ratio (CSR), the corresponding number of cycles at failure was determined. There was some dispersion in test results, therefore, upper and lower bound estimate curves are proposed. Considering a characteristic earthquake magnitude of about 7.5 the predicted equivalent number of cycles at failure according to Seed et al. [27] (as cited in Kramer [19]) would be of the order of 15. The corresponding CSR at failure is around 0.16 for the proposed lower bound profile

6. Seismic time histories

Seismic hazard was evaluated using a formal

defines ground motion for a postulated stiff soil outcrop with shear wave velocity from 200 to 375 m/s. Mean uniform hazard spectra (UHS) on stiff soil were defined for ALE and ELE design levels corresponding to 240 and 3,500 year periods, respectively.

The PSHA hazard curves were used to develop stiff soil spectra for 3,400 years (ALE). Following ISO recommendations, the ELE stiff soil spectra were computed dividing the ALE spectra ordinates by the seismic reserve capacity factor C_r , assumed to be 2.8. The equivalent return period for the ELE event is 240 years, which satisfies the ISO requirement of the minimum 200 year return period for this condition. Note that several approximations were required for the definition of return periods: the assessment was based on spectral period 2 s using simplified assumptions regarding the slope of the hazard curves.

Figure 4 shows UHS for stiff soil outcrop conditions. The data refer to the geometric mean of two components of horizontal ground motion computed for 5% damping. The corresponding spectral ordinates are listed in Table 5.

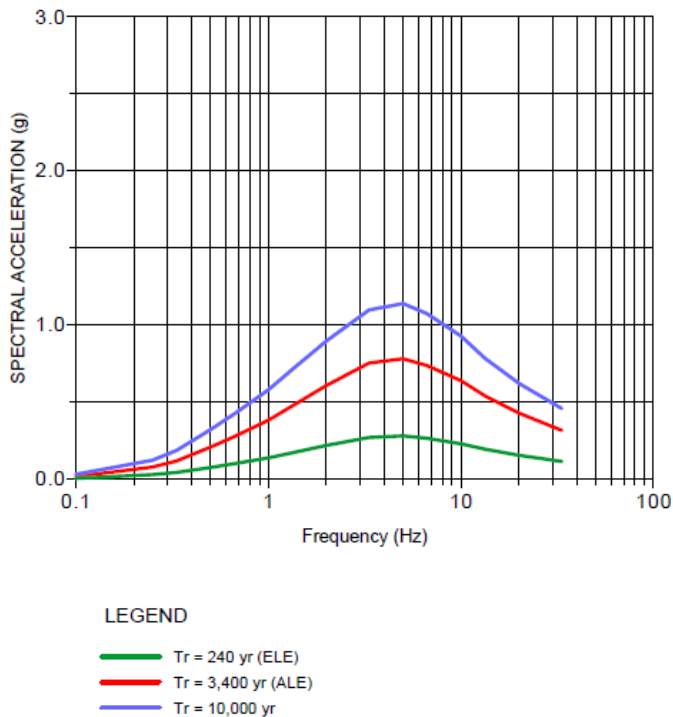


Figure 4: Stiff soil uniform spectra

A correction factor, C_c , is applied to a_R to account for the uncertainties that are not depicted in the seismic hazard curve. The values of C_c are found in Table 4

Table 5: 5% Damped Horizontal UHS, Stiff Soil Outcrop

| FREQUENCY(Hz) | PERIOD(s) | SPECTRAL ACCELERATION (g) | | |
|--------------------|-----------|---------------------------|-------|-----------|
| | | ELE | ALE | 10,000 yr |
| PGA (assumed 33Hz) | PGA | 0.112 | 0.314 | 0.456 |
| 20 | 0.05 | 0.152 | 0.426 | 0.619 |
| 13.33 | 0.08 | 0.192 | 0.538 | 0.781 |
| 10 | 0.1 | 0.227 | 0.636 | 0.926 |
| 6.67 | 0.15 | 0.262 | 0.734 | 1.071 |
| 5 | 0.2 | 0.278 | 0.779 | 1.137 |
| 3.33 | 0.3 | 0.268 | 0.751 | 1.096 |
| 2 | 0.5 | 0.216 | 0.606 | 0.895 |
| 1.33 | 0.75 | 0.169 | 0.474 | 0.711 |
| 1 | 1 | 0.136 | 0.38 | 0.578 |
| 0.67 | 1.5 | 0.098 | 0.274 | 0.422 |
| 0.5 | 2 | 0.073 | 0.205 | 0.319 |
| 0.33 | 3 | 0.041 | 0.116 | 0.184 |
| 0.25 | 4 | 0.027 | 0.076 | 0.12 |
| 0.1 | 10 | 0.002 | 0.014 | 0.03 |

6.1. Design time histories

A set of 7 suitable earthquake strong-motion time histories is selected for the nonlinear site response analysis. These earthquake records were chosen to cover the range of magnitude and distance of the hazard de-aggregation. All of the time histories were recorded on stiff soil sites per the PSHA. The normalized selected time histories provide coverage of the UHS on stiff soil as shown in Figure 5. All of the time histories were recorded on stiff soil sites per the PSHA. Table 6 lists the time history components used in the analysis.

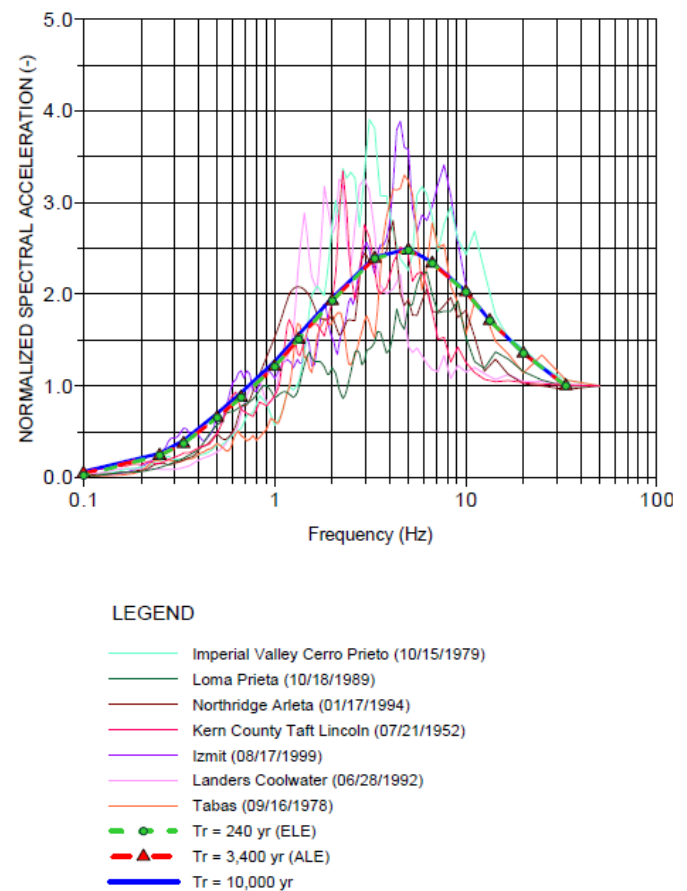


Figure 5: Normalised response spectra of time histories

6.2. Geotechnical model

The behavior of soil under cyclic loading is complex. In general soils exhibit, a nonlinear stress-strain response in that material stiffness decreases for increasing levels of strain. These effects are accentuated in seismic conditions as cyclic loading causes additional degradation of modulus and changes in pore-water pressures. Finally, the soil is inelastic for significant

strain levels, meaning that it exhibits different stiffness in loading and unloading conditions.

Table 6: Earthquake time histories for analysis

| EVENT | | STATION | | MAG | DIST (km) | COMP. | PGA (g) |
|----------------------------------|-----------------------------------|---------|--|-----|-----------|-------|---------|
| Kern County (USA) 07/21/1952 | Taft School Tunne | Lincoln | | 7.4 | 43.5 | Y | 0.18 |
| Loma Prieta (USA) 10/18/1989 | Saratoga-Aloha Ave | | | 6.9 | 27.6 | X | 0.51 |
| Northridge (USA) 01/17/1994 | Arleta-Nordhoff Ave. Fire Station | | | 6.7 | 9.9 | X | 0.34 |
| Tabas (Iran) 09/16/1978 | Tabas | | | 7.4 | 52.0 | Y | 1.10 |
| Imperial Valley (USA) 10/15/1979 | Cerro Prieto | | | 6.5 | 26.7 | X | 0.17 |
| Landers (USA) 06/28/1992 | Desert Hot Spring | | | 7.3 | 23.0 | X | 0.17 |
| Izmit (Turkey) 08/17/1999 | Goyunuk-Delvet Hastanesi | | | 7.6 | 73.0 | X | 0.14 |

This inelastic response leads to hysteretic damping, which is again dependent on the level of strain.

The main aspects of soil behavior under cyclic loading were modeled for the numerical analysis. The constitutive model's components include:

- stress-strain response for initial loading (backbone curve) represented by modified

Hyperbolic model;

- unloading-reloading behavior and hysteretic damping captured using an extended

Masing rule [21];

- modulus degradation in clays considering the number of load cycle and strain levels;

- pore pressure generation-modulus degradation model for sands correlated to energy

dissipation.

Specific details of the model are not discussed in this paper.

6.3. Site-specific response

The probabilistic seismic hazard assessment determines the earthquake ground motion for a competent stiff soil outcrop. Stiff soil conditions may be encountered at significant depth. The presence of soft sediments in the shallow soil profile will significantly modify ground shaking, amplifying, and/or de-amplifying motions depending on the specific frequency. Site response was evaluated using a nonlinear analysis performed with the DEEPSOIL software (Hashash et al., [11]). As illustrated in Figure 6 the soil profile is represented as a series of infinite horizontal layers overlying an elastic bedrock. The

individual soil layers are represented using a multi-degree of freedom lumped parameter model. Layer thicknesses were selected to ensure the model correctly represented soil behavior up to frequencies of at least 33 Hz. The nonlinear dynamic equation of motion is solved in the time domain using the Newmark β method.

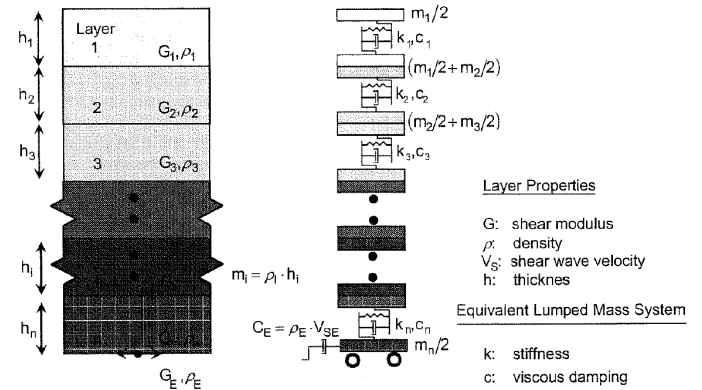


Figure 6: Lumped parameter model- From Hashash et al., [11]

Nonlinear soil behavior is represented using a pressure-dependent hyperbolic model (Konder and Zelasko [18], 1963; Matasovic and Vucetic [22 and 23]; Hashash and Park [12]. Energy losses are modeled with a combination of hysteretic damping utilizing a modified Masing [21] approach shown in Figure 7 (Darendeli [9]; Phillips and Hashash [25] and small strain Rayleigh viscous damping (Park and Hashash [24]).

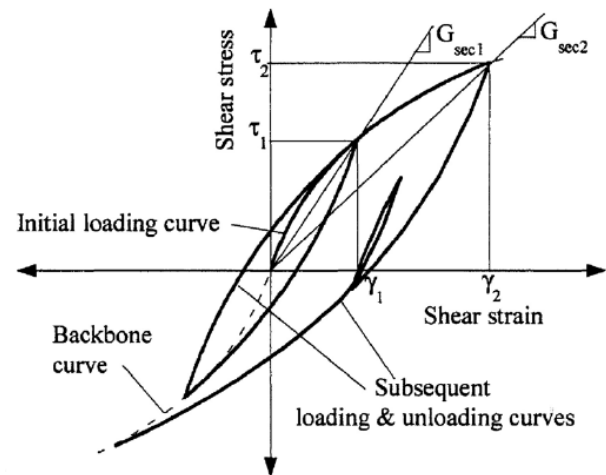


Figure 7: Hyperbolic model with extended Masing rule [21]- see Darandeli [9], and Phillips and Hashash [25]

The basic approach is to develop a numerical model of the soil column and subject it to an input competent outcrop ground motion. The input motion is assumed to consist of vertically propagating horizontal shear

waves. The dynamic response of the soil column is evaluated to find the motion at the ground surface. The response spectrum of ground motion at the ground surface is computed. The frequency-dependent spectral amplification ratio (SAR) is then computed for the record as:

$$SAR(f) = \frac{S_a(f)^{surface}}{S_a(f)^{input}} \quad (2)$$

SAR Spectral amplification ratio as a function of

$S_a(f)^{surface}$ Spectral acceleration at ground surface or mudline

$S_a(f)^{input}$ input equivalent outcrop ground motion

The 7 horizontal acceleration time-histories are propagated through the soil column, and SAR values are computed for each record. The average response of the soil column, considering the record to record variability, is represented by the mean of the SAR values from the individual records.

The stiff soil UHS is adjusted for the effects of site response using the mean SAR values. The response spectrum at the surface is computed as:

$$S_a(f)^{surface} = S_a(f)^{input} \times \overline{SAR(f)} \quad (3)$$

$\overline{SAR(f)}$ mean spectral amplification ratio as a function of frequency f

Formally, this approach should be applied to adjust individual frequency-dependent hazard curves, and the resulting response spectrum interpolated for the desired return periods. An acceptable engineering approximation is to factor the stiff soil UHS directly to obtain the motion at the mudline.

As site response is nonlinear with the level of the earthquake ground shaking, the SAR values must be defined as a function of the intensity of the input motion. For this study, SAR values have been defined for the target return periods by scaling the input time histories to the desired stiff soil PGA.

The vertical spectral acceleration at a period T according to ISO 19901-2 [14] should be half of the corresponding horizontal spectral acceleration. No additional reductions for water depth effects are considered.

The ISO approach was compared to the results of recent research regarding vertical spectra for both onshore and offshore locations. Several teams of researchers have addressed the issue of the ratio of vertical to horizontal spectral acceleration (V/H) for onshore locations. Bozorgnia and Campbell [4] examined the V/H ratio based on predictions of vertical and horizontal spectral acceleration from their previously developed attenuation laws (Campbell and Bozorgnia [8]. Gülerce and Abrahamson [10] performed a similar evaluation but regressing directly the V/H ratios using the

extensive NGA database of shallow crustal measurements. Bommer et al. [2] confirmed the Gülerce and Abrahamson's [10] results utilizing a different dataset of European and the Middle East events. The results of all three groups showed the ratio V/H to be less than one half for periods exceeding about 0.5 s. Higher ratios are expected onshore for shorter periods and events relatively near the site.

Boore and Smith [3] provide data applicable to offshore locations. They present the results of 20 years of monitoring of a network of submarine strong-motion stations. Field measurements show that the offshore time histories have very low vertical motions

In comparison with an average similar onshore site, especially in short periods. The Boore [3] data shows offshore V/H ratios of the order of 0.2 to 0.3 for short period motion (0.1 to 1.0 s). This is attributed primarily to the effects of the water column.

6.4. Mudline and in profile time histories

A set of seven 3-component earthquake time histories were produced. Data are provided for mudline and at depths of 15 and 30 m below seabed for ELE, ALE and 10,000 year return periods. Plots of the time histories. The data is not included in this paper.

The time histories were developed using the results of the non-linear site response analysis at the site. A set of seven stiff soil records are used for site response. These records are appropriately amplified using the DEEPSOIL nonlinear model to account for site conditions. The resulting mudline accelerograms were post-scaled to match the ELE and ALE year spectra over a period range considered appropriate for structural design. Horizontal components were matched in the range of 1.0 to 3.0 s, while vertical components were scaled to match from 0.5 to 0.75 s.

The methodology was as follows:

- Pre-scale horizontal components (x and y) of recorded (native) stiff soil time histories to target stiff soil PGA;
- Propagate pre-scaled stiff soil horizontal records through soil column using DEEPSOIL model to compute mudline response;
- Scale the horizontal components of motion at mudline to design spectrum over frequency range using FEMA 450 [20];
- Scale stiff soil vertical components directly to mudline vertical target design spectrum under the assumption that vertical motion is not significantly amplified;
- In-profile time histories were computed applying the scaling factors at mudline.

The procedure was repeated for the ELE and ALE ground motion.

6.5. Spectral Matching for Horizontal Components

The mudline time histories were scaled to match the design spectrum following FEMA 450 [20] recommendations. The input data consist of sets of

recorded earthquake ground motion (x, y, and z components). A group of seven 3-component records was selected and scaled such that the average response meets or exceeds the design spectrum over a range of periods near the fundamental period of the structure.

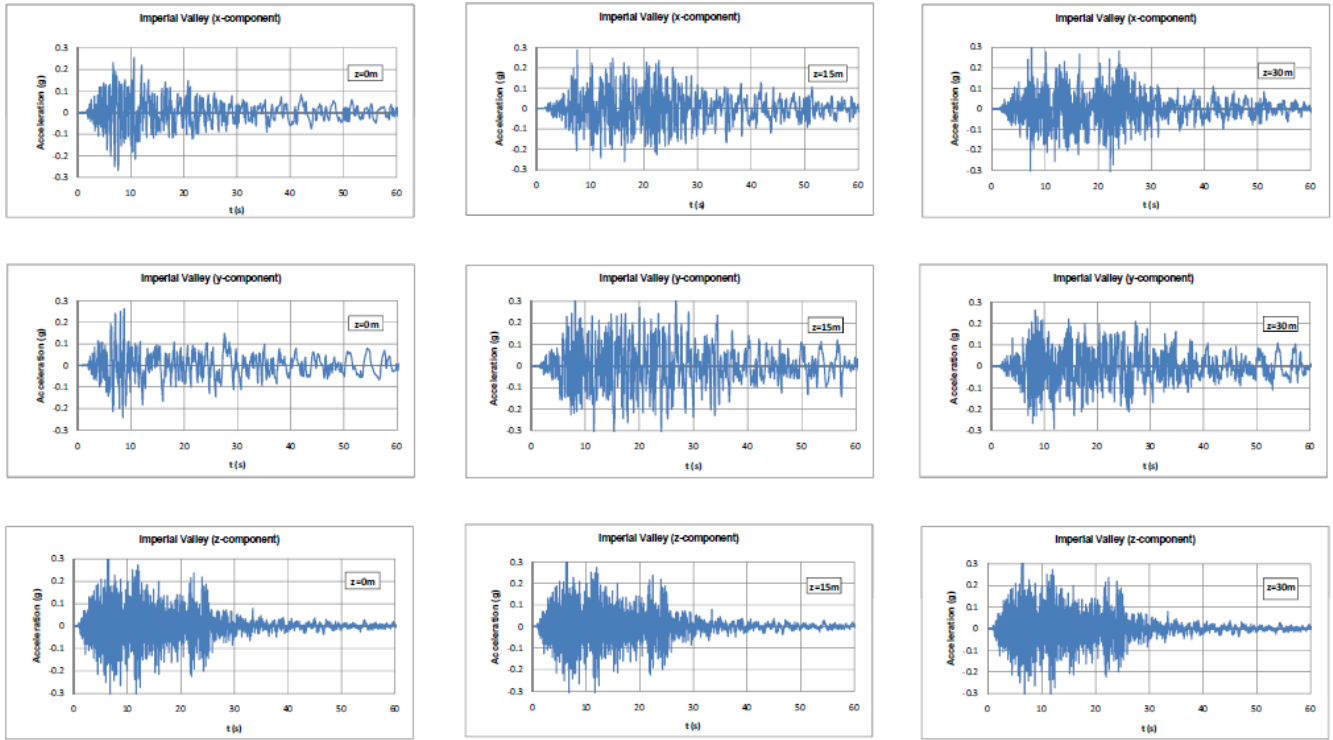


Figure 8: Imperial 10/15/79. Amplified acceleration time-histories- ALE

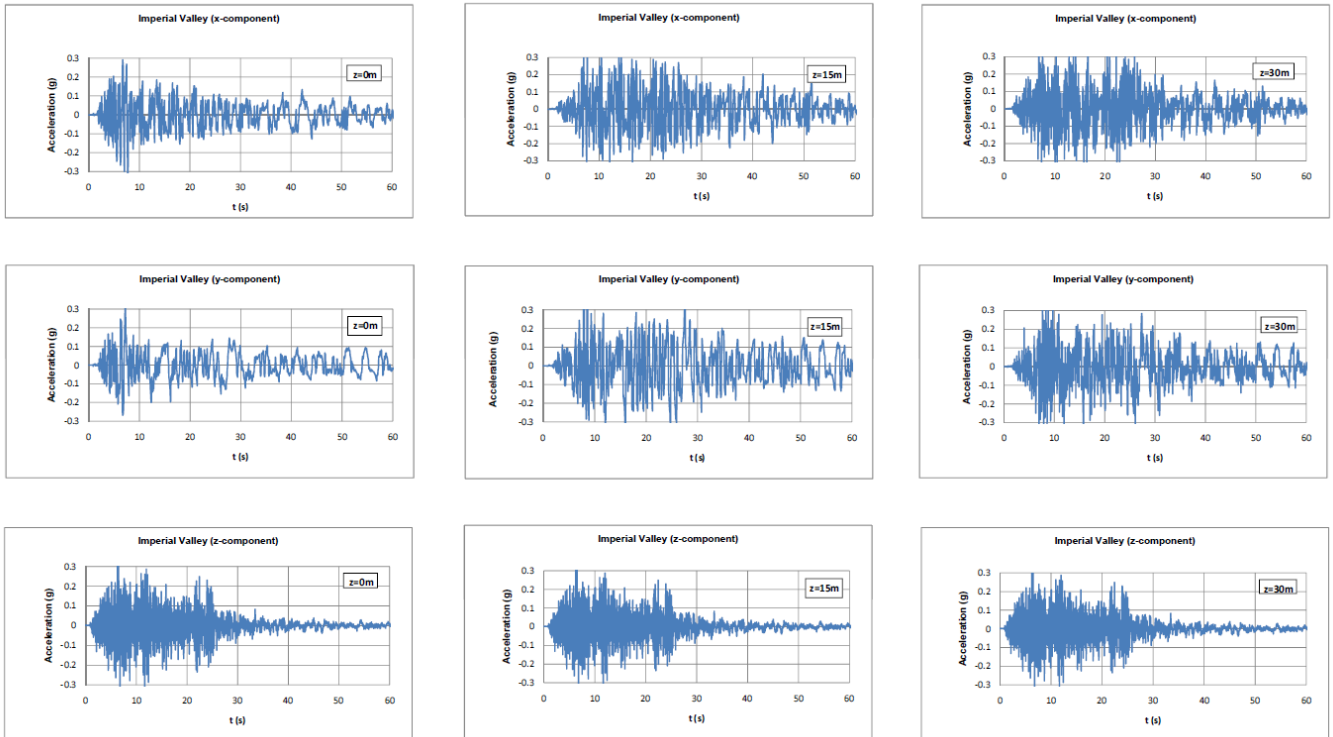


Figure 9: Imperial Valley, 10/15/1979 Amplified Acceleration Time History, 10,000yr Event

For 3D analysis, the horizontal components of each record are combined as a Square Root of Sum of

Squares (SRSS) spectrum. The SRSS spectrum is constructed by taking the square root of the sum of the

squares of the 5% damped response spectra, at each period (T) for the x and y components of ground motion.

Appropriate scaling factors are then selected for the individual time histories such that the average of the SRSS is not less than 1.3 times the corresponding ordinate of the design response spectrum. FEMA [20] requires that scaling criteria be satisfied for each period between 0.2 and 1.5 times the fundamental period of the structure. This criterion was relaxed somewhat, applying the period ranges discussed in Section 5.5.1. Note that the factor of 1.3 is required to account for the geometric difference between the design spectrum defined for a single direction and the SRSS which is a combination of two orthogonal components. The verification test can be summarized as follows:

$$\frac{\sum_1^n SF_i \cdot SRSS_i(T)}{n} \geq 1.3 Sa_{TD}(T) \quad (4)$$

Where

SF = scaling factor

$SRSS(T)$ = square root of the sum of squares of x and y of mudline response spectra;

$Sa_{TD}(T)$ = design spectral acceleration

T = periods considered in the range between 0.2 and 1.5 times fundamental period of the structure;

n = number of time histories considered

Two examples are given in Figures 8 and 9. Figure 10 shows the fit of the “Horizontal” scaled time histories.

7. Concluding remarks

This paper uses the ISO 19902 [16] methodology for deriving the site-specific earthquake time-histories using a refined coupled pore pressure generation-site response analysis. The design spectra and time histories are derived using modeling of the site response in effective stress instead of total stress to take into account the effect of soil liquefaction. It was decided that liquefaction is likely to occur in the first ten meters of the profile (which is a sandy layer) for the ALE and 10,000 year return periods. For the ELE event liquefaction development is marginal. The design spectra are given in Table 5. A different approach may lead to spectra which are somewhat lower for the ELE event, and higher for the ALE and 10,000 year return periods. The reduction of spectral acceleration at longer return periods reflects the effects of liquefaction.

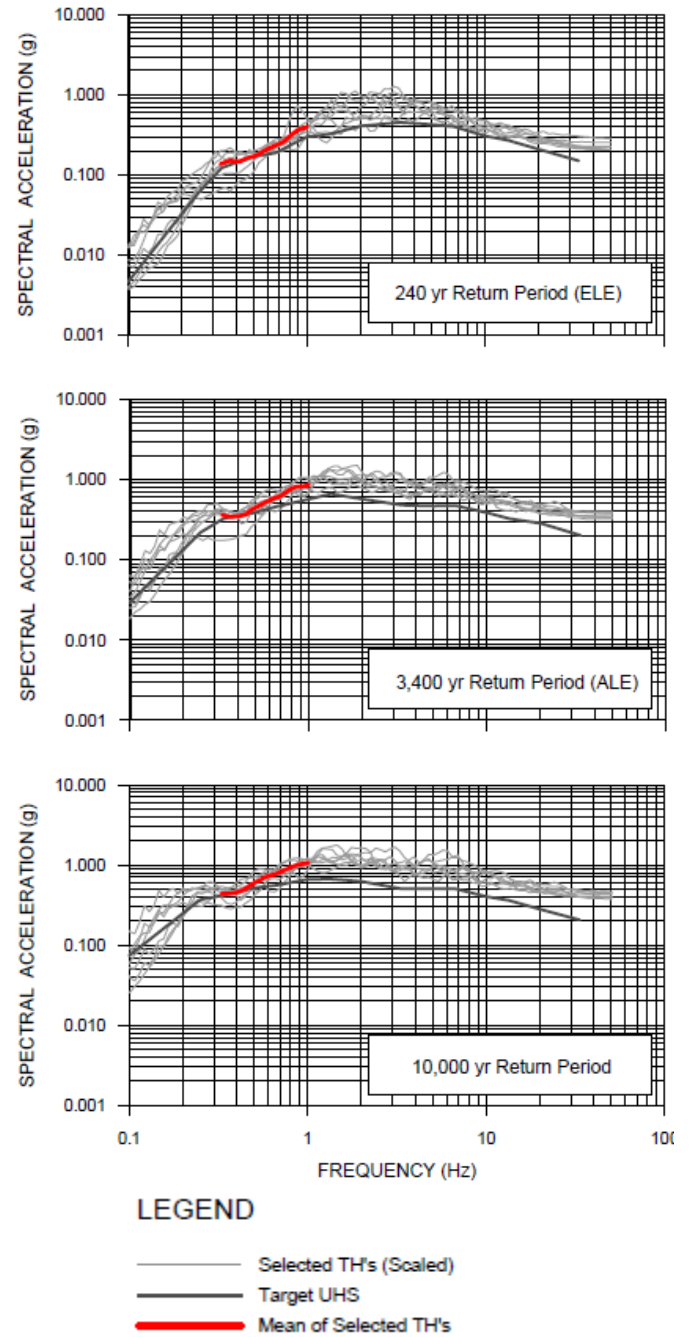


Figure 10: The “Horizontal” scaled time histories showing the fit of scaled time histories

A set of seven 3-component earthquake time histories were calculated for the manifold location. The time histories were obtained through effective stress site response analysis, and thus represent the soft soil conditions at the site in liquefaction conditions. Data are provided for mudline, 15 m, and 30 m penetration. These records have been scaled to match the design spectra in the range of fundamental frequency of the structure following the FEMA [20] procedure.

8. References

1. Banon, H, Cornell, A., Marshal, P.W., Nadim, F., and Younan. H., (2001), *ISO SEISMIC DESIGN GUIDELINES FOR OFFSHORE PLATFORMS*, OMAE2001/S&R-2114, 20th Offshore Mechanics and Arctic Engineering Conference – OMAE 2001, Rio de Janeiro, Brazil, 3rd – 8th June 2001
2. Bommer, J. J., S. Akkar, and O. Kale, (2011), *A Model for Vertical-to-Horizontal Response Spectral Ratios for Europe and the Middle East*, Bulletin of the Seismological Society of America, Vol. 101, No. 4, pp. 1783–1806.
3. Boore, D. M., and Smith, C.E., (1999), *Analysis of Earthquake Recording Obtained from the Seafloor Earthquake Measurement System (SEMS) Instruments Deployed off the coast of Southern California*, Bulletin of the Seismological Society of America, Vol. 89, No. 1, pp. 260–274.
4. Bozorgnia, Y. and Campbell, K.W., (2004), *The Vertical-to-Horizontal Response Spectral Ratio and Tentative Procedures for Developing Simplified V/H and Vertical Design Spectra*, Journal of Earthquake Engineering, Vol. 8, No. 2, pp. 175-207.
5. Cornell CA, Vanmarcke E.H., (1969), *The major influences on seismic risk* Proceedings of the 4th World Conference on Earthquake Engineering, Santiago, Chile.
6. Cornell CA., (1968), *Engineering seismic risk analysis*, Bulletin of the Seismological Society of America 58(5):1583–1606.
7. Cornell, CA, (1996), *Reliability-based earthquake resistant design; the future*, paper, No. 2166, 11th World Conference on Earthquake Engineering pp 1-11.
8. Campbell, K. W., and Y. Bozorgnia, (2003), *Updated near-source ground motion (attenuation) relations for the horizontal and vertical components of peak ground acceleration and acceleration response spectra*, Bulletin of the Seismological Society of America, Vol. 93, pp. 314-331.
9. Darendeli, M. B., (2001), *Development of a New Family of Normalized Modulus Reduction and Material Damping Curves*, Department of Civil Engineering, the University of Texas at Austin, Austin.
10. Gülerce, Z., and N. A. Abrahamson, (2011), *Site-Specific Design Spectra for Vertical Ground Motion*, Earthquake Spectra, Vol. 27, No. 4, pp. 1023–1047
11. Hashash, Y .M. A., D. R. Groholski, C. A. Phillips and D. Park, (2009), *DEEPSOIL V3.7beta, User Manual and Tutorial*, 88 pp.
12. Hashash, Y. M. A. and D. Park, (2001), *Non-linear One-Dimensional Seismic Ground Motion Propagation in the Mississippi Embayment*, Engineering Geology, Vol. 62, No. 1-3, pp. 185-206.
13. Idriss, I.M., Dobry R., and R.D. Singh, (1978), *Nonlinear Behaviour of Soft Clays During Cyclic Loading*, Journal of Geotechnical Engineering Div., ASCE, Vol. 104, No. 12, pp. 1427-1447.
14. International Standard ISO 19901-2, (2004), *Petroleum and Natural Gas Industries – Specific Requirements for Offshore Structures – Part 2: Seismic Design Procedures and Criteria*, November.
15. International Organization for Standardization: ISO 19901-4, (2002), *Petroleum and Natural Gas Industries – Specific Requirements for Offshore Structures – Part 4: Geotechnical and Foundation Design Considerations*.
16. International Organization for Standardization: “ISO 19902:2007(E) Petroleum and Natural Gas Industries – Fixed Steel Offshore Structures,” 2007.
17. Ishibashi, I., and X. Zhang, (1993), *Unified Dynamic Shear Moduli and Damping Ratios of Sand and Clay*, Soils and Foundations, Vol. 33, No. 1, pp. 182-191.
18. Konder, R. L. and J. S. Zelasko, (1963), *A Hyperbolic Stress-Strain Formulation of Sands*, Proceedings of the 2nd Pan American Conference on Soil Mechanics and Foundation Engineering, Sao Paulo, Brazil, pp. 289-324.
19. Kramer, S. L., (1996), *Geotechnical Earthquake Engineering*, Prentice Hall, Inc., Upper Saddle River, NJ.
20. NEHRP (2005), *Recommended Provisions for Seismic Regulations for New Building and Other Structures (FEMA 450)*, Prepared for Federal Emergency Management Agency, National Institute of Building Sciences, Washington, D.C. 4, pp. 1023–1047.
21. Masing G., (1926), *Eigenanspannungen und verfertigung beim messing*, Second International Congress on Applied Mechanism, Zurich, Switzerland, pp. 332-335.
22. Matasovic, N. O. and Vucetic, M., (1993), *Cyclic Characterization of Liquefiable Sands*, Journal of Geotechnical and Geoenvironmental Engineering, ASCE, Vol. 119, No. 11, pp. 353-69.
23. Matasovic, N. O. and M. Vucetic, (1995), *Generalized Cyclic-Degradation-Pore-Pressure Generation Model for Clays*, Journal of Geotechnical Engineering, Vol. 121, No. 1, pp. 33-42.
24. Park, D., and Hashash, Y.M.A., (2004), *Soil Damping Formulation in Nonlinear Time*

- Domain Site Response Analysis*, Journal of Earthquake Engineering, Vol. 8, No. 2, pp. 249-274.
25. Phillips, C., and Hashash, Y.M.A., (2009), *Damping Formulation for Non-Linear 1D Site Response Analyses*, Soil Dynamics and Earthquake Engineering, Vol. 29, No. 7, pp 1143-1158.
 26. Sadigh, K., Chang, C.-Y., Egan, J. A., Makdisi, F., and Youngs, R. R., (1997), *Attenuation relationships for shallow crustal earthquakes based on California strong motion data*, Seismol. Res. Lett. 68 1, 180–189.
 27. Seed, H. B., Idriss, I.M., Makdisi, F., and Banerjee, N., (1975), *Representation of irregular stress time histories by equivalent uniform stress series in liquefaction analyses*, EERC 75-29, Earthquake Engineering Research Center, University of California; Berkeley.
 28. Seed, H. B., Wong, R. T., Idriss, I. M., and K. Tokimatsu, (1986), *Moduli and Damping Factors for Dynamic Analyses of Cohesionless Soils*, Journal of Geotechnical Engineering, ASCE, Vol. 112, No. 11, pp. 1016-1032
 29. Scawthorn, Ch, and (Editor), Wai-Fah Chen, W.F., (2002) *Earthquake Engineering Handbook* CRC Press; 1 edition.
 30. Vucetic, M. and Dobry, R., (1991), “Effect of Soil Plasticity on Cyclic Response”, Journal of Geotechnical Engineering, ASCE, Vol. 117, No.1, pp. 89-107.
 31. Wells, D.L., Coppersmith, K.J, (1994), *New Empirical relationship among magnitude, rupture length, rupture width, rupture area, and surface displacement*, Bulletin of the seismological society of America, Vol, 84, No. 4 pp 974-1002, 1994.
 32. Yasseri, S, (2020), *Seismic Design of Subsea Jumper per ISO: Part I- Preliminaries*, IJCOE Vol.4/No. 1/Spring 2020 (31-43)
 33. Yasseri, S. (2020), *Seismic Design of Subsea Spool per ISO: Part III- Analysis & Design*, IJCOE Vol.4/No. 3/Autumn 2020

Table of abbreviations

| Abbreviation/ Acronym | Description |
|--------------------------|---------------------------------------------------|
| BSF | below seafloor |
| COG | Centre Of Gravity |
| CPT | Cone Penetration Test; |
| DLE | Ductility Level Earthquake |
| FE | Finite Element |
| FEMA | Federal Emergency Management Agency |
| FTA | Flowline Termination Assembly |
| G | Shear modulus |
| Gmax | Shear modulus at low strain |
| HP | High Pressure |
| NA | Not Applicable |
| NEHRP | National Earthquake Hazard Reduction Program |
| PEER | Pacific Earthquake Engineering Research Centre |
| PGA | Peak Ground Acceleration |
| PSHA | Probabilistic Seismic Hazard Assessment |
| RC | Resonant Column |
| Sa | Spectral Acceleration |
| SD | Slump Deposits |
| Su | Undrained shear strength |
| UHS | Uniform Hazard Spectra |
| Vs | Shear wave velocity |